The Company of Biologists

RESEARCH ARTICLE

Kinematic control of male Allen's hummingbird wing trill over a range of flight speeds

Christopher J. Clark[1],* and Emily A. Mistick[1,2]

ABSTRACT

Wing trills are pulsed sounds produced by modified wing feathers at one or more specific points in time during a wingbeat. Male Allen's hummingbirds (*Selasphorus sasin*) produce a sexually dimorphic 9 kHz wing trill in flight. Here, we investigated the kinematic basis for trill production. The wingtip velocity hypothesis posits that trill production is modulated by the airspeed of the wingtip at some point during the wingbeat, whereas the wing rotation hypothesis posits that trill production is instead modulated by wing rotation kinematics. To test these hypotheses, we flew six male Allen's hummingbirds in an open-jet wind tunnel at flight speeds of 0, 3, 6, 9, 12 and 14 m s^{-1}, and recorded their flight with two 'acoustic cameras' placed below and behind, or below and lateral to the flying bird. The acoustic cameras are phased arrays of 40 microphones that used beamforming to spatially locate sound sources within a camera image. Trill sound pressure level (SPL) exhibited a U-shaped relationship with flight speed in all three camera positions. SPL was greatest perpendicular to the stroke plane. Acoustic camera videos suggest that the trill is produced during supination. The trill was up to 20 dB louder during maneuvers than it was during steady-state flight in the wind tunnel, across all airspeeds tested. These data provide partial support for the wing rotation hypothesis. Altered wing rotation kinematics could allow male Allen's hummingbirds to modulate trill production in social contexts such as courtship displays.

KEY WORDS: Adventitious sound, Locomotion-induced sound, Sonation, Trochilidae, Wind tunnel

INTRODUCTION

Wing communication sounds are produced in flight by birds that include flappet larks (*Mirafra* spp.) (Norberg, 1991), manakins (Bostwick and Prum, 2003) and guans (Delacour and Amadon, 1973); fruit bats (Boonman et al., 2014); and insects such as butterflies (Yack et al., 2000), grasshoppers (Otte, 1970) and mosquitoes (Cator et al., 2009). In many of these examples, the wing sounds are produced only during displays, such that the communication sound is not also present in ordinary flight. But in some, such as mosquito wing hum (Cator et al., 2009), the communication wing sounds are simply a modulated version of a sound that is also produced during ordinary flight. One sound produced in ordinary flight is the topic of the present study: a sound called the 'wing trill' produced by males of some species of

[1]Department of Evolution, Ecology and Organismal Biology, University of California Riverside, CA 92521, USA. [2]Institute for Resources, Environment and Sustainability, University of British Columbia, Vancouver, BC, V6T 1Z4, Canada.

*Author for correspondence (cclark@ucr.edu)

C.J.C., 0000-0001-7943-9291

hummingbird (Clark, 2008; Feo and Clark, 2010; Hunter, 2008; Hunter and Picman, 2005).

Wing trills are distinctive, high-frequency sounds produced at one or more specific points in time during a wingbeat. Wing trill is not the low-frequency humming sound wings produce as an inevitable byproduct of flight for which hummingbirds are named. Rather, the wing trill is a specialized sound that is produced primarily or exclusively by males (i.e. it is sexually dimorphic) by modified wing morphology (Fig. 1A). Wing trills have evolved several times in hummingbirds (Clark et al., 2018). In addition to its presence in ordinary flight (Fig. 1B), the trill is a prominent feature of courtship displays that males direct towards females (Fig. 1C). When a female visits his courtship territory, a male of many of the species in the 'bee' hummingbird clade (Mellisuginae) uses altered wing kinematics to produce an acoustically modulated version of the wing trill during a close-range display called the shuttle display (Clark, 2016; Clark et al., 2011b; Feo and Clark, 2010). As a prominent feature of a sexually selected display for choosy females, the wing trill has likely evolved under female choice. We therefore sought to understand if it could serve to signal the male's flying ability.

Assessing what, if anything, the trill could signal to the female about the male's flight abilities required establishing the relationship between production of the trill and the kinematics of flight. The subject of the present study, male Allen's hummingbirds (*Selasphorus sasin sedentarius*; Grinnell, 1929), produces a loud 9 kHz wing trill with the subtly tapered tip of the outer wing feather, P10 (Fig. 1A,B; Movie 1). Casual observation of males flying about their courtship territories suggested several patterns that we sought to investigate. The trill substantially varies in sound pressure level (SPL) with mode of flight. Although audible in most flight, observation of wild birds suggested that the trill is accentuated during high-speed flight, courtship displays and maneuvers (Movie 1), and can be nearly inaudible during hovering. Thus, we sought to understand the basis for differences in trill production as a function of flight speed. It also seemed possible that trill production is partially voluntary (*sensu* Clark, 2016): when a territorial, breeding male leaves his perch to pursue a female, his trill often seems louder than in comparable flights that are not in response to a possible mate. Thus, we sought to assess the mechanisms underlying the trill, to determine whether and how males can adjust their wing kinematics to voluntarily enhance or suppress the trill.

The wing trill is a trill (i.e. a pulse train) rather than a continuous tone because it is not produced continuously during the wingbeat. It consists of a series of pulses of sound (Fig. 1B) usually produced at the same rate as the wingbeat frequency (Clark, 2008; Feo and Clark, 2010), although in some specific circumstances not relevant to the present study, it can instead be produced at twice the wingbeat frequency (Feo and Clark, 2010). Production once per wingbeat implies it is produced at a single position within the wingbeat cycle. Hereafter, we call the position and duration within the wingbeat in

1
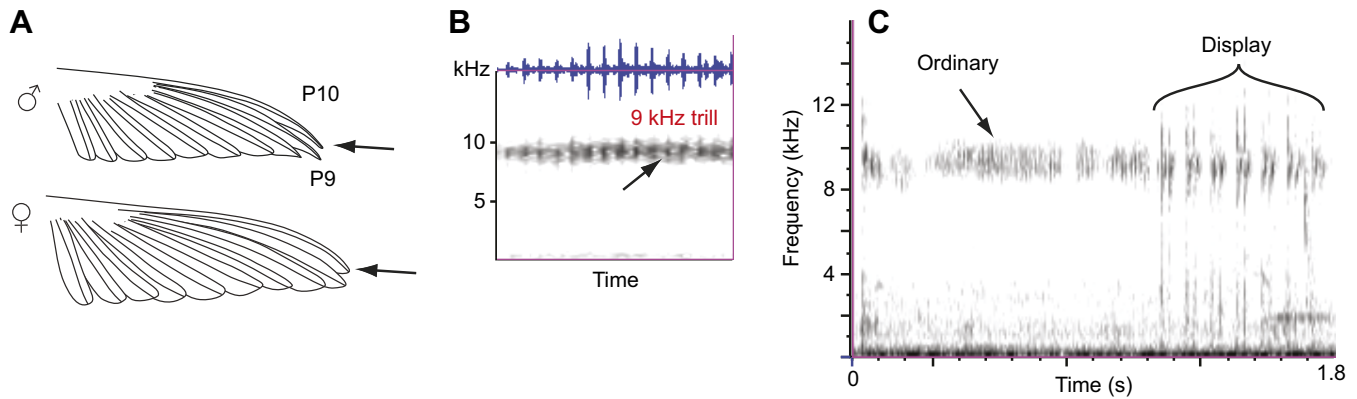
Fig. 1. Allen's hummingbird wing trill. (A) Wing of an adult male (top) and female (bottom) Allen's hummingbird (*Selasphorus sasin sedentarius*). Males produce a wing trill in flight with primary 10 (P10) and possibly P9, both of which have a tapered tip. Females do not produce the trill and lack the tapered tip (arrows). (B) Spectrogram (bottom) and waveform (top) of a male's wing trill, showing approximately 14 wingbeats. The trill has an acoustic frequency of approximately 9.0 kHz. (C) The trill is modulated during courtship displays such as the pendulum display (from Clark, 2016).

which the trill is produced, the 'trill duty cycle', and the corresponding velocity of the wingtip at the moment that the trill is produced, V_{trill}. V_{trill} is unknown, as the trill duty cycle is unknown. The duration of the duty cycle is not constant over varying modes of flight: Hunter and Picman (2005) found that the trill duty cycle is approximately 20% of the wingbeat during hovering, and increased as high as 32% of the cycle in other modes of flight in rufous hummingbird (*Selasphorus rufus*). We hypothesized that the trill duty cycle within the wingbeat is produced in the downstroke (Fig. 2A) because that is when unrelated birds such as the *Smithornis* broadbills (Clark et al., 2016), red-billed streamertail (Clark, 2008) or doves (Hingee and Magrath, 2009; Niese and Tobalske, 2016) produce their wing sounds. Alternative possibilities are mid-upstroke, or during pronation (the wing rotation prior to the downstroke) or supination (the wing rotation prior to the upstroke).

The physical source of sound determines how SPL may be modulated in different modes of flight. The source in a congener, the broad-tailed hummingbird (*Selasphorus platycercus*) is aeroelastic flutter of the tip of P10 (Clark et al., 2012; Miller and Inouye, 1983), in the narrowed region of the feather vane that is at the wing's tip. Allen's hummingbird P10 has a similar shape (Fig. 1A). There are at least three ways SPL could be modulated: (1) aeroelastic flutter of individual, isolated feathers usually (but not always) increases in SPL at higher airspeeds (V_{trill}) (Clark et al., 2011a,b), likely due to an increase in the amplitude of flutter (Clark et al., 2013a); (2) changes in wingtip geometry – for example, changes in the overlap between neighboring feathers (P10 and P9) – could also affect SPL by, for example, controlling the surface area of P10 that is free to flutter; and (3) any mechanism that causes a change in the trill duty cycle could produce changes in time-averaged SPL by simply extending the duration over which the sound is produced. These three hypothetical mechanisms are not mutually exclusive and could interact; for instance, changes in overlap between neighboring feathers could affect trill duty cycle duration as well as surface area.

These prior findings suggest a simple hypothesis of how the trill is modulated according to mode of flight: the wingtip velocity hypothesis, in which trill production co-varies with wingtip velocity (Fig. 2A). The wing trill is simply modulated by V_{trill}; flight kinematics in which V_{trill} is higher are louder, for any of the mechanisms mentioned above. V_{trill} is unknown, so we tested this hypothesis by estimating the maximum wingtip velocity during the wingbeat, V_{max}, and assumed that V_{max} and V_{trill} are correlated.

An alternative hypothesis is the wing rotation hypothesis: pronation or supination modulates trill production (Fig. 2A). For example, similar to the wingtip velocity hypothesis, wing rotation could affect the onset of flutter (and thus the trill duty cycle length), or could affect bending and overlap of the tips of the outer wing feathers, or both. According to this wing rotation hypothesis, the wing trill will co-vary with aspects of wing kinematics other than V_{trill}. We tested these two hypotheses by flying birds at different airspeeds within a wind tunnel, because V_{max} is higher during high-speed flight than it is in hovering (Tobalske et al., 2007), and on account of our anecdotal observations that the trill seemed more pronounced in high-speed flight.

Testing these two hypotheses required accounting for a spatial effect: the sound field is potentially directional (Fig. 2A). For instance, the wing hum of hovering flies and mosquitoes is distinctly directional (Arthur et al., 2014; Sueur et al., 2005). The source of sound is apparently flutter of P10. We recently showed that a fluttering feather may be a dipole-like, highly directional sound source with the axis of the dipole oriented relative to the anatomical orientation of the feather (Clark and Mistick, 2018). If the sound field of the trill is also directional, then changes in SPL apparent at a single point could be the result of a reorientation of the sound field, rather than changes in SPL at the source. For example, in hovering flight, the anatomical stroke plane angle (β; Fig. 2A) is near zero, whereas in high-speed forward flight the anatomical stroke plane is rotated to nearly 90 deg relative to horizontal. If the sound field is directed relative to β, it could (for instance) have highest SPL below the bird during hovering, but highest SPL horizontally behind the bird during high-speed forward flight. Therefore, we recorded from multiple locations around the bird, to test the hypothesis that SPL changes as a function of position around the bird.

MATERIALS AND METHODS
Aeroacoustic wind tunnel
Most studies of bird flight employ an 'Eiffel' style suction wind tunnel in which the animal flies in an enclosed working section upstream from the fan. While it is easy to enclose the working section with optically transparent material such as plastic, it is more difficult and expensive to make the working section sides out of acoustically transparent material (Debrouwere, 2013; Remillieux et al., 2008). It is possible to use an aerodynamic nose cone to place microphones directly in the unidirectional flow of a closed working section (Clark et al., 2013a,b; Soderman and Allen, 2002); however, reverberation within this enclosed space will interfere with precise
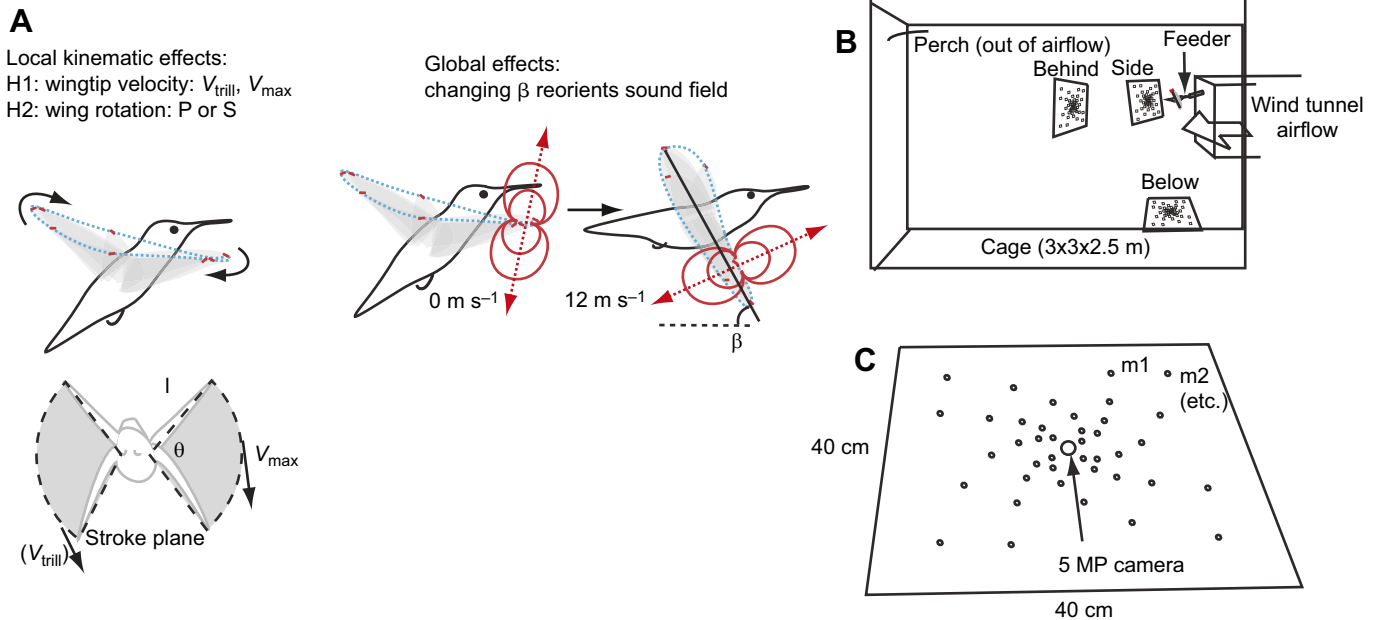
Fig. 2. Hypotheses and methods. (A) Two types of hypotheses (H) were tested: local and global. Local kinematic effects: trill production could be modulated by wingtip speed at the moment the trill is produced (V_{trill}). While V_{trill} is unknown, it is likely correlated with V_{max}, the maximum wingtip velocity. Alternatively, it could be modulated by wing rotation [pronation (P) and/or supination (S)]. l, wing length; θ, stroke amplitude. Global kinematic effects: changes in kinematic orientation (such as changes in the anatomical stroke plane angle, β) could re-orient the sound field (red). (B) Experimental setup (not to scale). Three acoustic camera placements (behind, side and below), each 0.5 m from the bird at the feeder. The camera in the 'below' position did not move. The other acoustic camera was placed either in the 'behind' or 'side' orientation. The only feeder available was in the mouth of the open jet of the wind tunnel. The flow impinged directly onto the camera in the 'behind' position (side is lateral to the flow). For further diagrams of the tunnel, see Fig. S1. (C) The acoustic cameras were 40×40 cm spiral arrays of 40 microphones (m1, etc.), surrounding a 5 megapixel camera.

measurement of SPL. Another solution is to place the working section of a suction tunnel inside a pressure-sealed room, allowing it to be open, but this was beyond our budget. The economical solution was to construct a blower wind tunnel following the design of Sarradj et al. (2009), in which the bird flies in an open jet of air, and microphones are placed close to the animal and far from reflective surfaces.

Our tunnel design was copied, with modifications, from Sarradj et al. (2009). The biggest design difference is that their tunnel was circular in cross-section (E. Sarradj, personal communication), whereas ours is square, in order to accommodate a ∼90 cm (36 in) working section that was not used in this study (Fig. S1). Our goal was a tunnel capable of 30 m s^{-1} with a cross-section of 35.6×35.6 cm^2 (14×14 in, where 1 in is 2.54 cm), a volumetric flow of 4 m^3 s^{-1}, with an estimated total pressure drop of <1000 Pa. The total length available was 13.3 m: 4 m for the jet and 9 m for the tunnel itself. Air entering the tunnel first flows through two parallel HVAC silencers [Vibro Acoustics RD-MV-F9, Markham, ON, Canada; ∼274 cm (108 in) length], which attenuate the fan and motor sound that propagates upstream. The centrifugal fan (HDAF-240, Cincinnati Fan, Mason, OH, USA) has a maximum volumetric flow of approximately 4.2 m^3 s^{-1}. The motor (induction, 10 HP, Baldor VM3714T, ABB, Fort Smith, AR, USA) driving the fan is direct-drive and controlled by a variable-frequency drive inverter. The default drive frequency of 4 kHz produced distinct motor noise in the test section at 4 and 8 kHz, plus a couple of sideband frequencies, whereas setting the drive frequency to 16 kHz resulted in negligible motor sound in the working section, when the diffuser–silencer (described next) was attached.

After leaving the fan, air traveled down a short duct and through a vibration isolation boot, then entered into a large diffuser–silencer.

Within the diffuser–silencer, the air travels around a large angled insert as shown in Fig. S1B. This insert prevented direct transmission of sound from the fan in a straight line down the tunnel to the working section, instead forcing all fan noise to reflect off multiple sound-absorptive surfaces. Both the insert and walls of the tunnel (gray areas in Fig. S1) were lined with acoustic batting (recycled cotton) with a high noise-absorption coefficient, which was covered with flat perforated sheet metal with an open area of ∼50% (a convoluted surface, as is typical for anechoic chambers, would cause turbulence in the fast-flowing air of a wind tunnel). The cross-sectional area of the diffuser–silencer increased continuously down its length, expanding from ∼91×91 cm to ∼163×163 cm (36×36 in to 64×64 in). The air then traveled through a ∼10 cm (4 in) honeycomb [hole diameter: ∼5 cm (0.2 in)] and three pressure screens (open area: 64%) each separated by ∼10 cm (4 in), followed by a contraction section that contracted from ∼163 to ∼36 cm (64 to 14 in; contraction area ratio of 20:1). The air then exhausts into the lab as a jet.

The bottom of the jet was 0.86 m above the floor, and one side was 1.02 m from a wall, both of which reflect sound and were not acoustically treated. The diffuser–silencer and intake both project through a wall that separated the test room from the motor room, which greatly reduced transmission of fan and motor noise to the jet via open air. The main background sound is of the jet itself, particularly the shear layer (i.e. the layer of turbulent air bounding the jet, lying between the laminar flow of the jet on the inside and the still air of the lab on the outside), as well as objects placed in flow. Airspeed was calibrated with a hot-wire anemometer. We recorded background sound of the tunnel with a B&K 4189 1/2 in microphone outfitted with a B&K UA 0386 nosecone (Brüel & Kjær, Nærum, Denmark) using the same recording equipment as described in Clark et al. (2013b).

Animal experiments

Six wild male Allen's hummingbirds were captured on the University of California, Riverside, campus in December 2016 to February 2017, which is shortly after the annual molt (the trill is loudest at this time of year). Handling the birds and holding them in captivity tended to cause them to lose the trill because the very tip of the wing is abraded by collision with the cage walls as the bird adjusts to captivity. Therefore, we sought to minimize handling and duration in captivity. We captured males early in the day, immediately introduced them into the experimental chamber, trained them to visit the feeder, and collected all of the data in one day, rather than housing the birds for several days. We aborted data collection on individuals that seemed to lose or reduce their ability to produce the full trill. After the experiment, each male was banded and then released.

We constructed a large cage (roughly 3 m×3 m×2.5 m) around the mouth of the jet, lined with bird netting and with perches near the top, where the birds preferred to perch, out of the airflow. The only available feeder was a 10 ml syringe placed in the mouth of the jet, such that the bird had to fly in the airflow in order to feed. The feeder was filled with dilute (10%) nectar to encourage frequent feeding.

When the bird flew to the feeder, we recorded its flight with either two high-speed cameras (Miro EX4, Vision Research, Wayne, NJ, USA) to record average 2D wing kinematics (N=4 males) or two 'acoustic cameras' (described below). One high-speed camera was placed laterally to the bird to record stroke-plane angle (relative to horizontal) and wingbeat frequency. The other camera was placed to record wing stroke amplitude: underneath the bird at low airspeeds or behind the bird at high airspeeds. Birds were flown at 0, 3, 6, 9, 12 and 14 m s^{-1}, presented in a randomized order for two acoustic camera setups: either with an acoustic camera 50 cm lateral to the bird (position 'side') or with an acoustic camera 50 cm behind the bird ('behind'). The second acoustic camera was placed 50 cm below the bird ('below') and remained in place (Fig. 2B), as a reference throughout all trials. We repeated flight recordings at each of six airspeeds with both camera setups 3 times each (36 feeding bouts per individual, where a feeding bout is the approach, feeding and departure from the feeder). We did not record data for any feeding bouts that lasted less than 0.5 s. Most feeding bouts lasted several seconds. To reduce within-sample variation, each feeding bout recorded by the acoustic cameras was subsampled 3 times (0.5 s each) from near the beginning, middle and end of the feeding bout. These three values were averaged, and this bout average was used as a sample for statistical analysis.

Acoustic cameras

The bird was recorded with two microphone arrays (SIG ACAM 100 Microphone Array, OptiNav Inc., Bellevue, WA, USA; www.optinav.com), or 'acoustic cameras' for short. Each array consisted of 40 microphones arrayed in a 40 cm×40 cm spiral (24 bit, 50 kHz sampling rate, flat response at 60 Hz to 15 kHz), with an optical 5 megapixel camera (frame rate: 24.45 Hz) integrated in the middle of the array. The acoustic cameras were attached via USB to laptop computers, and run with OptiNav BeamformX software (version 2.06). This software used a proprietary beamforming technique (Dougherty et al., 2013) to generate a spatial 'heat' map on the camera image of acoustic SPL for a 1/3 octave band centered at 9 kHz. We set the decay time (similar to a fast Fourier transform window size) of 0.5 s, and a focal distance of 0.5 m (i.e. matching the distance between the camera and the bird), except where indicated otherwise in figure captions. The focal depth at this

distance was approximately ±20 cm. Most background sound within the lab (such as fan and motor noise from the wind tunnel) did not fall within this focal plane, and thus was not represented in the sound map.

Acoustic calibration

We tested the factory calibration of the acoustic cameras in a quiet auditorium with background SPL levels of ~35 dB SPL (whole A-weighted spectrum). We played tones at 2, 4 and 8 kHz at three amplitudes each from a speaker that was 1.6 m away from the acoustic cameras, as well as two SPL meters, and a calibrated B&K 4189 microphone (as per the calibration in Clark et al., 2013b). These measurements indicated that the acoustic cameras were accurate to within 2.1±3.9 of SPL (re. 20 µPa) (mean±s.d.), and returned values of approximately 1.5 dB different from each other (presented data have had this offset removed).

We then calibrated for the effects of the wind tunnel. When the tunnel is running, it potentially affects acoustic recordings in four ways: (1) background sound produced by the fan, motor and airflow varies with speed; (2) the shear layer of the tunnel theoretically distorts the sound such as by causing spectral broadening (Debrouwere, 2013) and by slightly shifting downstream the apparent source location (although these effects should be slight at airspeeds far below Mach=1); (3) the jet impinges on the acoustic camera itself in the 'behind' recording position; and (4) self-noise from turbulent flow shed by the syringe feeder, and sometimes the shear layer, was present within the focal plane at airspeeds above 9 m s^{-1}. We calibrated for the first three effects by placing a small speaker in the airflow, directly facing each camera, and playing a test tone of 9.0 kHz, with the wind tunnel set to each airspeed (0, 3, 6, 9, 12, 14 m s^{-1}), repeated at 25 and 35 dB, where 35 dB was approximately the same SPL as the wing trill of the birds as measured by the acoustic camera. The cameras returned the same acoustic SPL (±1.5 dB) of sound from the speaker, irrespective of airspeed or camera position (orientation), indicating that the first three effects are negligible.

Effect 4 (self-noise from the feeder) was not an issue for camera positions below and to the side of the bird, because the sound produced by the feeder did not spatially overlap with sounds produced by the bird. For the camera position behind the bird, we placed the feeder next to the speaker (so that its flow-induced noise was added to that of the speaker). This did not appreciably change the measured SPL of the sound from the speaker, indicating that effect 4 was also negligible for sounds above 25 dB.

Statistics

We separately digitized stroke plane angle (β) from lateral high-speed videos and stroke amplitude (θ) from the video from below or behind the bird (from an average of 10 beats). Assuming the wingtip moves under simple harmonic motion, peak wingtip velocity (V_{max}) during hovering is simply $\pi l\theta f$, where l is the wing length of 0.04 m and f is wingbeat frequency. When the bird is flying in the tunnel, the wing's motion is superimposed on top of the freestream flow (U). We estimated the maximum wingtip velocity (V_{max}) in the airflow as:

$$V_{max} = \sqrt{(\pi l\theta f)^2 + 2U\pi l\theta f \cos\beta + U^2}. \quad (1)$$

We tested the effects of airspeed and orientation in a linear model within the program JPM Pro 12.0.1. We assessed how acoustic SPL varied with airspeed, using a general linear model with bird (random factor), camera position, airspeed (U_{air}), U_{air}^2 and two interaction

terms: camera position$\times U_{air}$ and camera position$\times U_{air}^2$. The U_{air}^2 term was included to model effects with respect to airspeed as a parabola, as many aspects of flight, such as the power curve, are known to have a U-shaped relationship with airspeed (Clark and Dudley, 2010). The position$\times U_{air}$ and position$\times U_{air}^2$ terms were to test whether SPL varied with airspeed differently in the different camera positions at low U_{air} and/or high U_{air}^2 speed, as predicted by the sound field reorientation hypothesis.

This research was conducted under appropriate US Fish and Wildlife Service, California Department of Fish and Wildlife, and bird banding permits; and with approval from the University of California, Riverside, Institutional Animal Care and Use Committee.

RESULTS

Average kinematics for four male Allen's hummingbirds flying at six airspeeds (0, 3, 6, 9, 12, 14 m s^{-1}) are presented in Fig. 3. With increasing airspeed, stroke amplitude (θ) declined (Fig. 3A); stroke plane angle (β) increased (Fig. 3B) and wingbeat frequency (f) was essentially unchanged (Fig. 3C). As a result, the maximum wingtip velocity (V_{max}) as estimated from Eqn 1 was approximately flat (at 16.5 m s^{-1}) at airspeeds of 9 m s^{-1} and below, whereas maximum wingtip velocity rose to ~19.5 m s^{-1} at airspeeds of 12 and 14 m s^{-1} (Fig. 3D).

In total, we obtained 430 acoustic camera recordings from 215 feeding bouts, recorded at six airspeeds (Movies 2 and 3). Data were evenly split between the two sampling locations (one camera below, one camera behind versus one camera below, one camera to the side). As there did not seem to be any systematic differences in the two setups, all data were pooled for a single statistical model. All males for which we present data seemed to maintain a strong trill for the entire duration of the experiment. As mentioned above, birds can show a decrease in the trill SPL over time; moreover, birds with reduced trill can sometimes regain it, e.g. if the feather barbs become realigned through preening. To test for possible order effects (e.g. changes in trill SPL that we did not notice), initial general linear model (GLM) analyses included the order of data collection as a covariate. Order was not significant ($P=0.12$), implying that trill SPL did not vary systematically throughout the experiment. Thus, sample order was not included in the final GLM analysis.

The full statistical results of the GLM are given in Table 1. Trill SPL varied with U_{air} ($P<0.0001$) and U_{air}^2 ($P<0.0001$), indicating that the trill SPL first decreased then increased with increasing airspeed (Fig. 4). Relative to acoustic camera position, neither acoustic camera position$\times U_{air}^2$ interaction term was significant ($P=0.20$, 0.16), suggesting that at high airspeeds, trill SPL did not increase at different rates in the different positions we recorded around the bird. By contrast, both acoustic camera position$\times U_{air}$ interaction terms were statistically significant, indicating that changes in trill SPL at low airspeeds do vary with position.

Two aspects of the data in Fig. 4A appear to be associated with changes in the stroke plane angle (β). At hovering, the trill had highest SPL below the bird, when the stroke plane was nearly horizontal. At higher airspeeds, the SPL behind the bird increased more quickly relative to the other two orientations, at the same time that the stroke plane was closer to vertical. Finally, the SPL was lowest lateral to the bird at all airspeeds except 0 and 3 m s^{-1}, when SPL behind the bird was not substantively different from SPL below the bird. These data support the global reorientation hypothesis (Fig. 2): the sound field was oriented relative to the stroke plane angle (β), such that it was louder in the axis perpendicular to the stroke plane. The effect size of this was moderate, approximately 4 dB (Fig. 4A).

The trill SPL did vary with speed (Fig. 4A,B), and the highest flight speeds had both higher V_{max} and higher trill SPL than for hovering (Fig. 4C). However, it became apparent that the data shown in Fig. 4 were not the primary explanation as to why trill SPL varies in different modes of flight. When the males maneuvered to approach or depart from the feeder, their trill was far louder, often by 20 dB or more (Fig. 4D), than in the steady-state flight at the feeder that we measured (Fig. 4A,B; Movies 2 and 3).

This maneuvering effect was present at all airspeeds; Fig. 5 presents an example from 0 m s^{-1} (Movie 2) while Fig. 6 presents similar data for 14 m s^{-1} (Movie 3). Each figure shows a series of panels (A–I in Fig. 5; A–L in Fig. 6) that are the acoustic camera sound maps from the three positions, at three different points in time: before, during and after feeding. A blob of color corresponds to the camera's localization of the sound in that frame, and warmer colors indicate louder sounds.

The acoustic camera recordings allowed an estimate of the location of the trill within the wingbeat, particularly with a shorter decay time of 0.1 s (which provided increased temporal resolution). At high flight speeds, in all videos examined, the trill was produced when the wings were below the bird's body. That is, the location of the trill implied it was produced sometime between the second half of the downstroke and the first half of the upstroke (Fig. 7A). This was often clearest when the birds maneuvered in to visit the feeder, when the wing trill was loud. The pattern for hovering is less clear (Fig. 7B), but is consistent with the pattern at high flight speeds. In three out of six birds, the source was broadly distributed and was not centered on any single part of the beat (Fig. 7Bii,v,vi) whereas in three other birds, the source was located at the part of the stroke plane corresponding to supination, similar to the videos at high airspeeds.
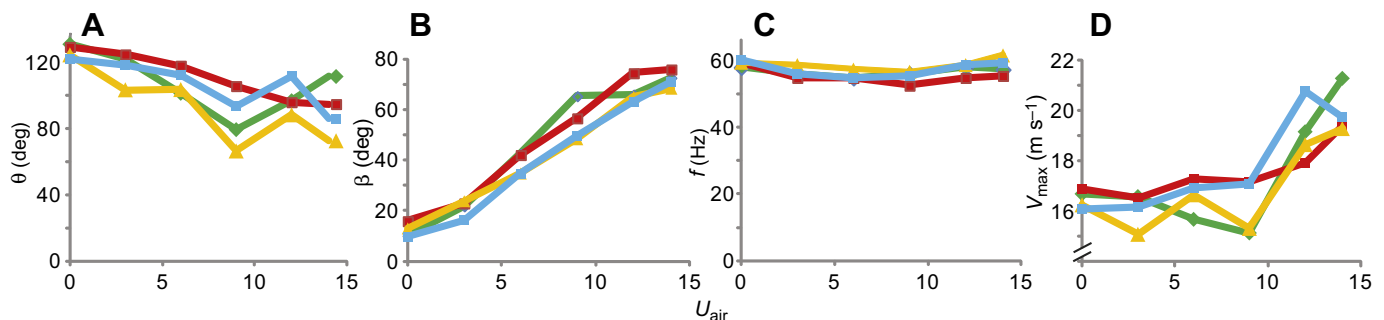
Fig. 3. Forward flight kinematics of $n=4$ male Allen's hummingbirds (*Selasphorus sasin sedentarius*) in a wind tunnel. (A) Stroke amplitude (θ), (B) stroke plane angle (β; as in Fig. 1C), (C) wingbeat frequency (f) and (D) estimated maximum wingtip velocity (V_{max}), calculated according to Eqn 1, as a function of airspeed (U_{air}). Each value is an average from 10 wingbeats. Note the truncated y-axis in D.

Table 1. General linear model of wing trill sounds as a function of U_{air}, acoustic camera position (Fig. 2B), and bird identity

| Variable	Estimate (±s.e.)	d.f.	t-ratio	P
Intercept	12.5±0.67	9.6	18.50	<0.0001
U_{air}	0.53±0.035	416	14.9	<0.0001
U_{air}^2	0.11±0.0088	416	12.9	<0.0001
Position (behind)	0.64±0.40	416	1.6	0.11
Position (below)	1.44±0.34	416	4.21	<0.0001
Behind×U_{air}	0.26±0.052	416	4.92	<0.0001
Below×U_{air}	−0.17±0.044	416	−3.83	<0.0001
Behind×U_{air}^2	−0.017±0.013	416	−1.27	0.20
Below×U_{air}^2	0.015±0.011	416	1.4	0.16

U_{air}, airspeed. Bird identity ($n=6$ birds) was included as a random variable: P-values 0.10, 0.03*, 0.35, 0.85, 0.025*, 0.38. *Statistically significant individual birds (individual bird curves shown in Fig. 4B).

DISCUSSION

How is the Allen's hummingbird wing trill produced? We present two principle findings. The first is that the sound field is directional and reorients with changes in flight speed (Fig. 4), although the magnitude of this effect was relatively weak. This makes it unclear whether this directionality has much biological relevance, a point

we return to in the second half of the Discussion. Second, contrary to our *a priori* expectations, the data presented here appear to better support the wing rotation hypothesis rather than the wingtip velocity hypothesis of trill production. There are three lines of evidence suggesting this conclusion: (1) the wing trill did not become substantially louder at higher airspeeds (Fig. 4A,C), (2) the substantial increase in trill SPL during maneuvers relative to steady-state flight at the feeder was irrespective of flight speed (Figs 5 and 6) and (3) as inferred, the trill is produced during or near wing supination, rather than midway through the upstroke or downstroke (Fig. 7). Each of these lines of evidence has caveats, as we discuss next.

According to the wingtip velocity hypothesis, we predicted that the trill in flight at high airspeeds would be substantially louder than in hovering, because peak V_{max} is greater at these speeds. Instead, the changes in SPL with airspeed were modest (Fig. 4); SPL at 12 m s^{-1} had essentially the same value as SPL at hovering, with slight differences in different recording positions, which are likely the product of changes in the anatomical stroke plane angle and sound field directionality (Fig. 4). These data weakly support the wing rotation hypothesis. According to this hypothesis, the U-shaped relationship between airspeed and wing trill SPL
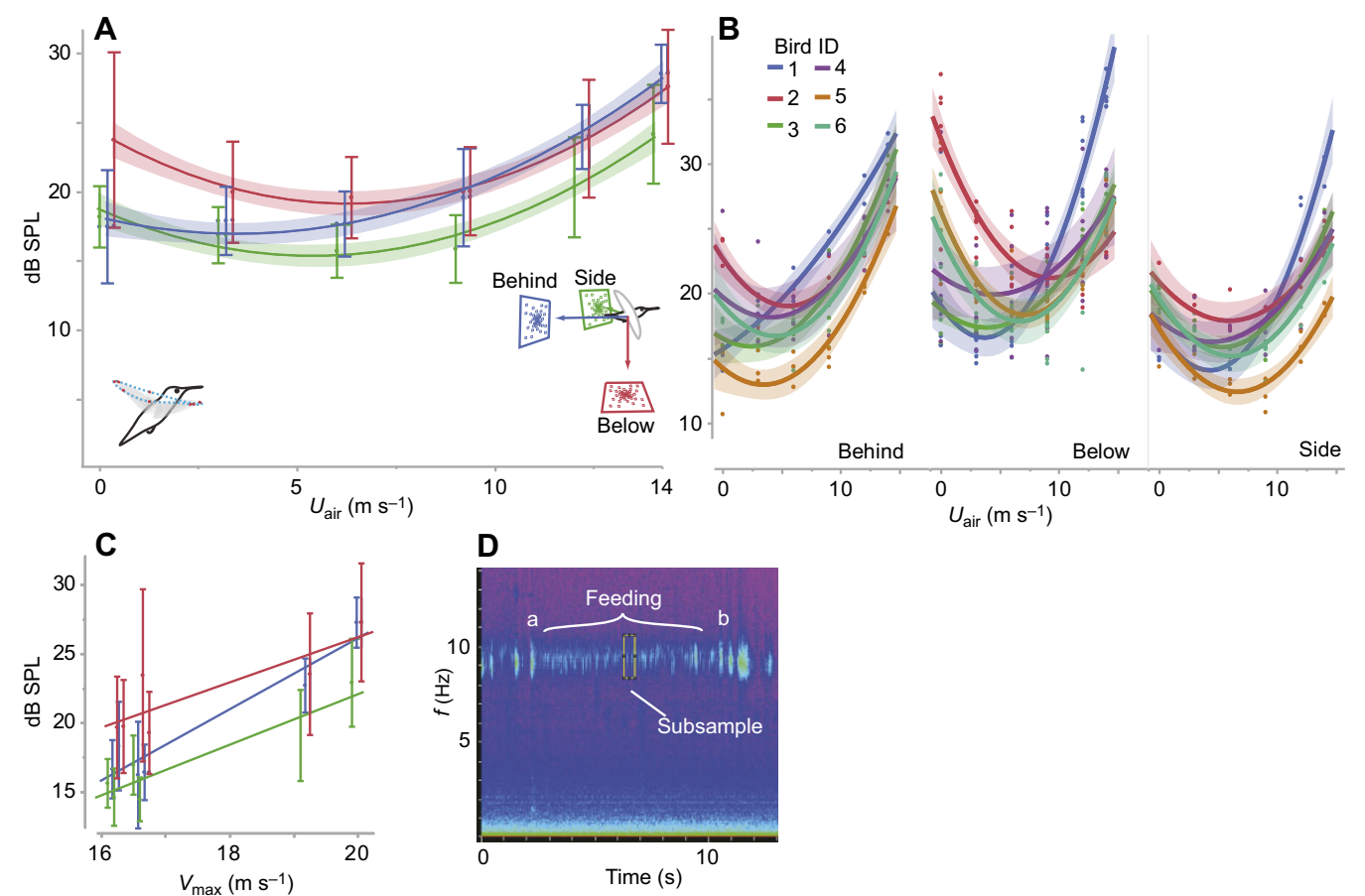

Fig. 4. Trill sound pressure level (SPL) during steady-state flight at a feeder, as a function of airspeed (U_{air}). (A) SPL (re. 0.5 m) as a function of position, averaged across all individual birds ($n=6$ birds). Means±s.d., with best-fit quadratic (shading: 95% confidence interval). Points are slightly offset in the x-axis to facilitate visualization of error bars. (B) SPL as a function of airspeed, plotted for each individual bird (individual samples shown). Note the truncated y-axis. (C) Trill SPL against average estimated maximum wingtip velocity (V_{max}; from Fig. 3D). Means±s.d.; points are slightly offset in the x-axis; lines are least-squares regression. (D) Spectrogram of a feeding bout, from one acoustic camera microphone. During the bout, the bird approaches the feeder (a), feeds and then departs from the feeder (b). During approach and departure, bird position was uncontrolled and varied. The boxed area shows a 0.5 s subsample; for each bout, three subsamples were recorded and averaged.
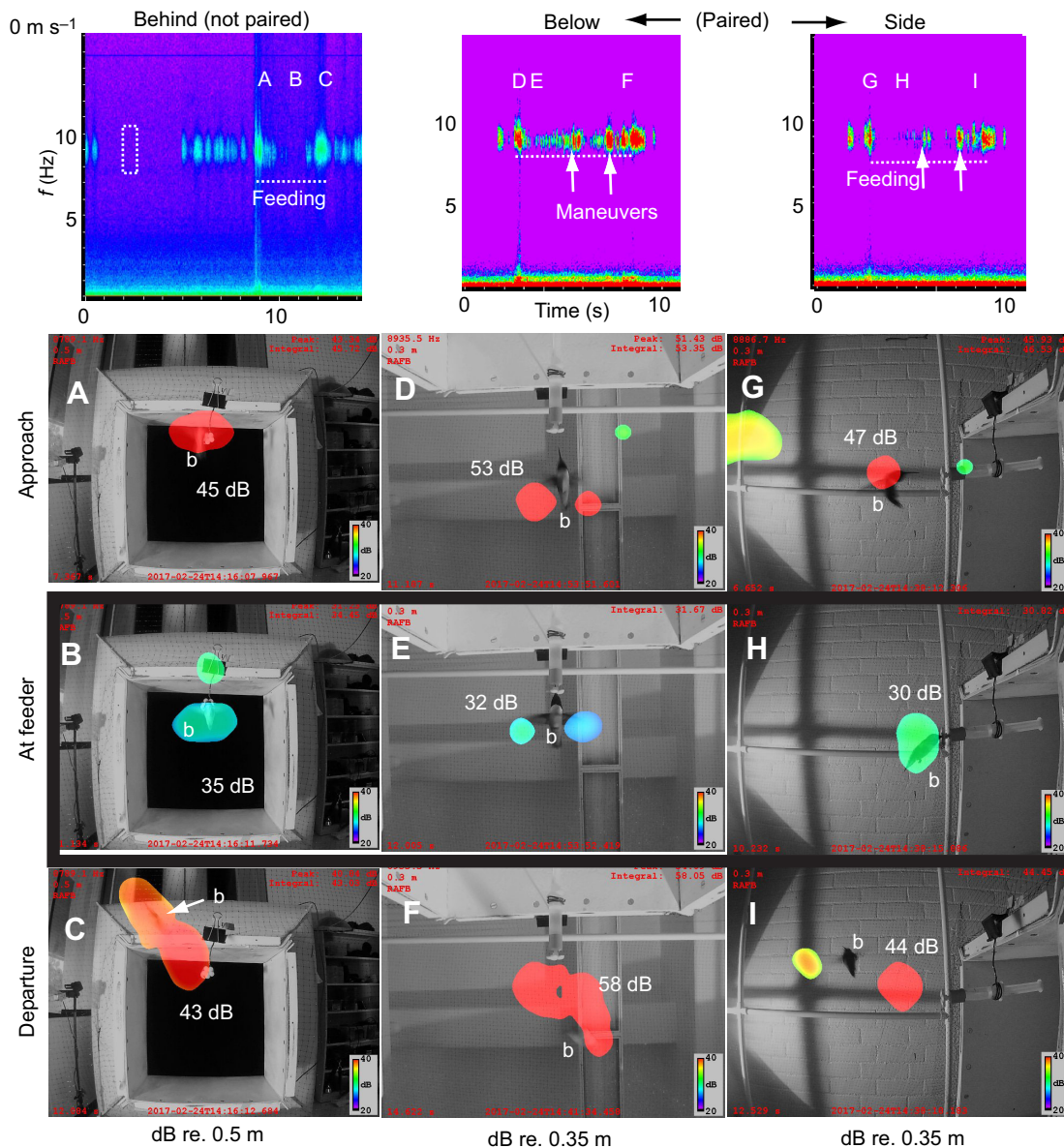
Fig. 5. Acoustic camera recordings of wing trill during a feeding bout at an airspeed of 0 m s⁻¹. The trill is louder during approach (A,D,G) and departure (C,F,I) from the feeder than it is during steady-state flight at the feeder (B,E,H). Top: spectrograms of approach, feeding and departure from the feeder, showing the 9 kHz wing trill. Dotted lines indicate the duration of the entire feeding bout. The box indicates the sample window used in beamforming (1/3 octave band centered at 9 kHz, 0.5 s integration window). The bird is labeled 'b'. 'Behind' is a separate feeding bout, whereas 'Below' and 'Side' are paired recordings from the same bout from different orientations. Arrows indicate interruptions to the feeding bout, in which the bird retracted and then reinserted its head into the feeder. Heat map lower threshold: 20 dB; dynamic range: 20 dB. A, D and G show the trill during a maneuver as the bird approaches the feeder. B, E and H are trill SPLs during steady-state feeding at the feeder, and correspond to the type of data presented in Fig. 4. C, F and I show the trill during a maneuver as the bird departs from the feeder.

(Fig. 4) is caused by an unmeasured aspect of wing kinematics that changes as a function of flight speed. However, this conclusion is tempered by the observation that the maximum wingtip velocity increased with flight speed less than we had expected. The increase in V_{max} between flight at 0 and 12 m s⁻¹ was only 1.2-fold, from approximately 16 to 19 m s⁻¹ (Fig. 4C). Tests of single feathers in airflow suggest that a change of airspeed of 3 m s⁻¹ should result in at most a 3–6 dB increase in SPL (Clark et al., 2013b), similar to the increase in SPL in Fig. 4C. Moreover, our wind tunnel data indicating that flight at high speed is not much louder than hovering (Fig. 4) contrasts with our anecdotal observation of wild birds flying at high speed and producing a loud trill, which motivated this study. We develop a possible explanation for this discrepancy below.

The second line of evidence supporting the wing rotation hypothesis is the data indicating the wing trill is far louder in maneuvers, often by more than 20 dB (Figs 5 and 6), than in steady-state flight at the feeder. As this was true at all camera orientations and flight speeds (Figs 4, 5 and 6), this difference in SPL was not attributable to changes in orientation of the sound field, or the changing, uncontrolled distance between bird and camera during approach or departure maneuvers. Rather, this difference in SPL must be attributable to some difference in wing kinematics of maneuvers, relative to the wing kinematics of steady-state flight while feeding at the feeder. A significant component of maneuvers is changes in wing rotation kinematics (Altshuler et al., 2012; Cheng et al., 2016); thus, the change in SPL during maneuvers is consistent with the wing rotation hypothesis.
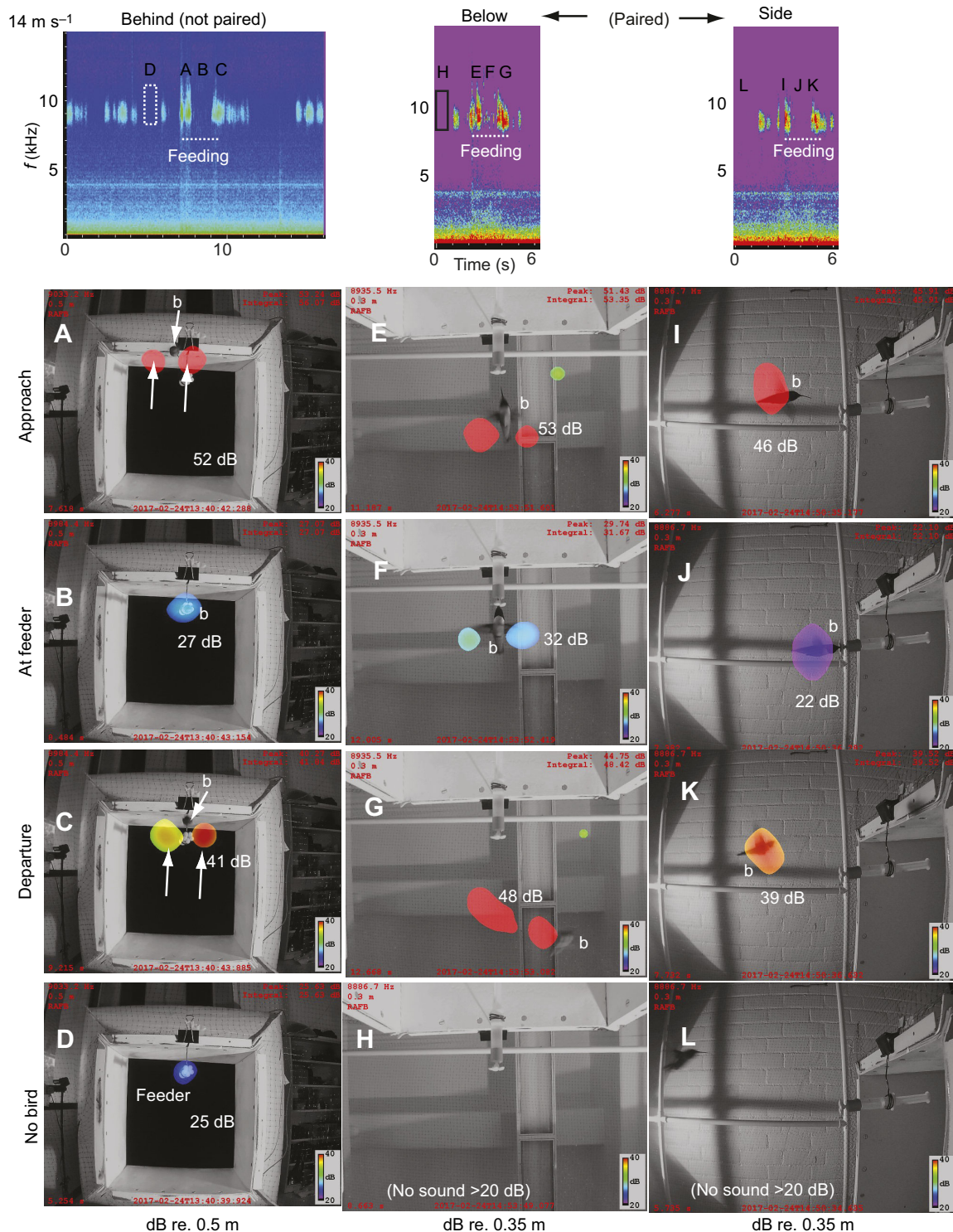
Fig. 6. Acoustic camera recordings of wing trill during a feeding bout at an airspeed of 14 m s⁻¹. The trill is louder during approach (A,E,I) and departure (C,G,K) from the feeder than it is during steady-state flight at the feeder (B,F,J). Top: spectrograms of approach, feeding and departure from the feeder, showing the 9 kHz wing trill. Dotted lines indicate the duration of the entire feeding bout. Boxes indicate the sample window used in the beamforming (1/3 octave band centered at 9 kHz, 0.5 s integration window). The bird is labeled 'b'. 'Behind' is a different bout, whereas 'Below' and 'Side' are for the same bout from different orientations (focal distance: 0.3 m). Heat map lower threshold: 20 dB. D, H and L show acoustic camera recordings with no bird present. The feeder produces self-noise (25 dB in this instance) in D, whereas self-noise is below the 20 dB threshold in H and L. Note that trill SPL in B is barely higher than feeder self-noise in D. B, F and J are trill SPLs during steady-state feeding at the feeder, and correspond to the type of data presented in Fig. 4.

Our third line of evidence supporting the wing rotation hypothesis comes from our acoustic camera sound maps, which suggest that the trill is produced just before, during or after wing supination (Fig. 7), and not wing pronation. These data were relatively consistent for flight at 12 m s⁻¹, as the reconstructions shown in Fig. 7A are for the birds as they approached or departed the
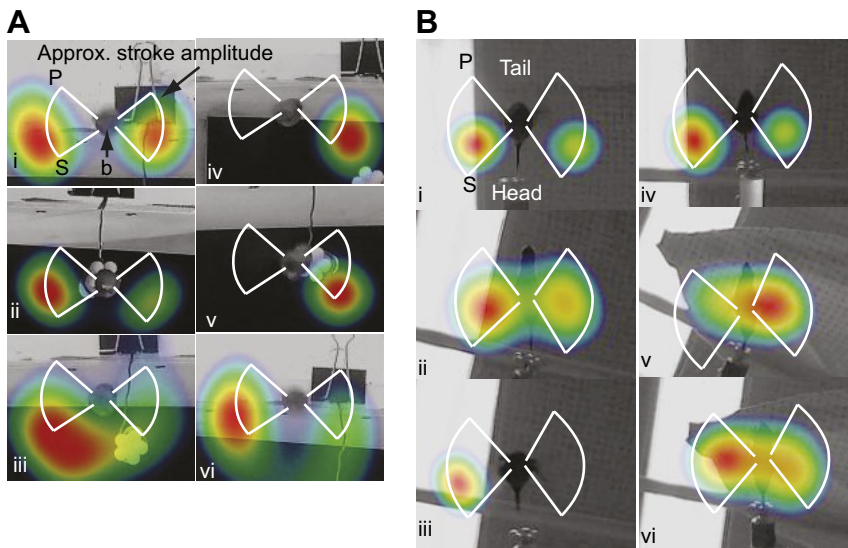
Fig. 7. Male Allen's hummingbird wing trill is produced during wing supination. Trill source location (heat map) in high-speed flight (A) and hovering (B) for n=6 birds. White outline is the approximate stroke plane angle, as estimated from wing blur in the video. P, pronation; S, supination; b, bird. (A) Acoustic camera images from high-speed flight (12 m s^{-1}, camera is behind the bird as it flies into the jet). All six images suggest the source is below the bird's body, approximately corresponding to supination. (B) Acoustic camera images during hovering (camera is below the bird); the source is either broadly distributed (ii,v,vi) or in front of the bird (i,iii,iv), approximately corresponding to supination. Acoustic camera settings used here maximize spatial resolution. Dynamic range of the heatmap is 3 dB, meaning that if one wing is >3 dB louder than the other, only one wing appears as a source. Scale is different in each image. Decay time of 0.1 s is shorter than in the main experiment, and reduces lag between bird position and acoustic reconstruction. Images Ai, iii, iv and vi are from relatively steady flight near the feeder, rather than at the feeder itself.

feeder slowly, and the trill was loud and thus provided a consistent signal (Fig. 7A). By contrast, reconstructions from hovering (Fig. 7B) were less clear. The reconstructions for hovering were all taken as the bird hovered at the feeder itself, and not during approach or departure, as in still air the birds approach or depart the feeder so rapidly that multiple wingbeats do not spatially overlap, and thus a beamforming image spanning multiple overlapping wingbeats was not possible. The reconstructions shown in Fig. 7Bii, v,vi suggest sound came from the middle of the wing and middle of the stroke, as opposed to Fig. 7Bi, iii and iv, which suggest sound came from near supination. The conditions leading to this reconstruction are not entirely clear, as the sound is produced by the wingtip (Fig. 1A), not the middle of the wing. Given the 0.1 s decay time of the beamforming used for this analysis and a wingbeat frequency of ~60 Hz (Fig. 3C), the acoustic position represented by the beamforming is an average over at least six wingbeats (or more, considering roll-off effects). Given that the trill was not particularly loud during hovering (Fig. 4), if the trill were produced at somewhat different positions from one individual wingbeat to the next, and especially if trill onset or cessation varied erratically from beat to beat, the time-averaged sound map might not represent any individual wingbeat. This interpretation of the data for 0 m s^{-1} suggests that the data at 12 m s^{-1} are also more representative of the production of the trill.

What are the possible underlying mechanisms that cause maneuvers to be >20 dB louder than in steady-state flight? Considering the three mechanisms mentioned in the Introduction – (1) increased airspeed (V_{trill}), (2) changes in the overlap between neighboring feathers caused by bending or (3) increased trill duty cycle – a 20 dB increase in SPL cannot be caused by either the first or third mechanisms in isolation. Hunter and Picman (2005) found that the trill duty cycle increased in maneuvers by roughly 50%. Even a doubling of trill duty cycle length would at most increase the time-averaged SPL by ~6 dB, if all else were equal. Another mechanism that is unlikely (in isolation) is increased V_{trill}. Low-speed maneuvers in still air can entail wing stroke amplitudes that approach 180 deg (Cheng et al., 2016; Clark, 2010); assuming θ=180 deg and no change in f, Eqn 1 predicts a V_{max} of ~24 m s^{-1} during a maneuver, which is 3 m s^{-1} greater than the highest V_{max} we measured in flight at an airspeed of 14 m s^{-1} (Fig. 3D). But, a 3 m s^{-1} difference in V_{trill} should by itself increase SPL by up to

6 dB (steepest slope in fig. 4A of Clark et al., 2013b) and so, even if V_{max} or V_{trill} are greater in a maneuver than in the experiment conducted here, this effect by itself probably cannot explain a 20 dB increase. Moreover, an increase in V_{trill} or V_{max} does not explain why trill SPL was high when the birds approached the feeder at high airspeeds (Fig. 7). At high airspeeds, the birds often approached the feeder slowly relative to a lab coordinate system. Their anatomical stroke amplitude during this approach did not seem much different from that in steady-state flight at the feeder (e.g. Fig. 7), suggesting it is unlikely that their V_{max} during approach much exceeded the V_{max} we estimated from steady-state flight behind the feeder (Fig. 3D). In total, changes in V_{max} or V_{trill} are unlikely to explain the elevated SPL during maneuvering (Fig. 6). The remaining hypothesis for the increase in SPL in maneuvers is changes in wingtip geometry that are induced by an unidentified aspect of supination kinematics. For example, altered timing or angular velocity of supination could change the amount of overlap between neighboring feathers P10 and P9, thus freeing a greater surface area of P10 to flutter. This does not rule out a role for altered V_{trill}, in combination with supination kinematics. In summary, we hypothesize that the dramatically louder trill in maneuvers is produced by an unidentified geometric change in the wingtip.

Wing trill function
The sound field as we measured it is somewhat directional though the magnitude of this directionality is low (of the order of 3–5 dB: Fig. 4), implying that males have some capacity to aim the sound towards the receiver. For example, according to the data in Fig. 4A, hovering above a female is louder than hovering at the same distance in front of her. Likewise, in a high-speed chase, the wing trill is potentially projected in front of and behind the flying bird, and thus automatically aimed towards a rival.

We define voluntariness as the degree to which an animal can modulate its kinematics and the ensuing sounds, while independently engaged in another, underlying behavior, such as a maneuver or accelerating from a perch (Clark, 2016). It is difficult to say how voluntary a wing trill could be, as it remains an open question which kinematic variables of the avian wing stroke are most constrained (least voluntary) and which are under the greatest voluntary control. What we propose next is a hypothesis and it is in

need of further study. We suggest that, because trill production is tied to supination, males may have partial voluntary control over the trill. The reason we suggest this is, given a bird has decided to fly a certain maneuver, we hypothesize that it is easier for the birds to voluntarily alter their wing rotation kinematics than it is to modulate stroke amplitude. As maneuvers and acceleration entail production of unbalanced forces, and wing-generated forces are modulated by wing velocity more than any other single kinematic variable (lift is proportional to V^2), we hypothesize that wingtip velocity may be the least-voluntary kinematic variable available for a bird to modulate the sound. Although wing rotation also affects force production (Dickinson et al., 1999), this is to a lesser degree; thus, the birds may have a greater degree of flexibility to voluntarily alter wing supination kinematics. For example, they might modulate its exact timing within the stroke, or angular velocity during supination, giving them some degree of strategic control over the trill, and enabling them to accentuate or suppress trill production. While they likely do not have complete voluntary control of the trill (the wing must be supinated every time it is flapped), this model explains our anecdotal observation that trill SPL seems to vary with social context. By altering supination kinematics, males may be able to fly relatively stealthily while encroaching on another male's territory, or loudly when chasing a potential mate. This explanation also seems to resolve the discrepancy between our anecdotal observation that high-speed flights may be loud in the wild but were relatively quiet in the controlled experimental conditions in the lab. In the lab, the birds had no motivation to produce a loud trill, whereas in the wild, high-speed flight is most often associated with agonistic interactions (fleeing and pursuits) with other hummingbirds. One avenue for further research would be to document the behavioral contexts in which wild males vary their trill SPL. For example, do males modulate their trill SPL in response to playback of another male's trill?

In courtship displays for females, the male produces a loud version of the trill that is modulated by altered wing kinematics (Clark et al., 2011b). Does the trill signal male flight performance? Our motivation for this study was our hypothesis that the trill SPL would be functionally connected to wingtip velocity, and thus to the production of flight forces. However, the data instead suggest that trill production is modulated by wing supination kinematics rather than by wingtip velocity. We have just argued that the sound is partially voluntary, which suggests that trill SPL may have fewer connections to flight ability of the male. One aspect of flight that the trill does nevertheless indicate to a receiver is wingbeat frequency, as the repetition rate of the trill is intrinsically the wingbeat frequency.

Data availability
Acoustic camera videos are available from the authors upon request.

Supplementary information
Supplementary information available online at
http://jeb.biologists.org/lookup/doi/10.1242/jeb.173625.supplemental

References
Altshuler, D. L., Quicazán-Rubio, E. M., Segre, P. S. and Middleton, K. M. (2012). Wingbeat kinematics and motor control of yaw turns in Anna's Hummingbirds (*Calypte anna*). *J. Exp. Biol.* **215**, 4070-4084.

Arthur, B. J., Emr, K. S., Wyttenbach, R. A. and Hoy, R. R. (2014). Mosquito (*Aedes aegypti*) flight tones: Frequency, harmonicity, spherical spreading, and phase relationships. *J. Acoust. Soc. Am.* **135**, 933-941.

Boonman, A., Bumrungsri, S. and Yovel, Y. (2014). Nonecholocating fruit bats produce biosonar clicks with their wings. *Curr. Biol.* **24**, 2962-2967.

Bostwick, K. S. and Prum, R. O. (2003). High-speed video analysis of wing-snapping in two manakin clades (Pipridae: Aves). *J. Exp. Biol.* **206**, 3693-3706.

Cator, L. J., Arthur, B. J., Harrington, L. C. and Hoy, R. R. (2009). Harmonic convergence in the love songs of the dengue vector mosquito. *Science* **323**, 1077-1079.

Cheng, B., Tobalske, B. W., Powers, D. R., Hedrick, T. L., Wethington, S. M., Chiu, G. T. C. and Deng, X. (2016). Flight mechanics and control of escape manoeuvres in hummingbirds. I. Flight kinematics. *J. Exp. Biol.* **219**, 3518-3531.

Clark, C. J. (2008). Fluttering wing feathers produce the flight sounds of male streamertail hummingbirds. *Biol. Lett.* **4**, 341-344.

Clark, C. J. (2010). Effects of tail length on an escape maneuver of the Red-billed Streamertail. *J. Ornithol.* **152**, 397-408.

Clark, C. J. (2016). Locomotion-induced sounds and sonations: mechanisms, communication function, and relationship with behavior. In *Vertebrate Sound production and Acoustic Communication*, Vol. 53 (ed. R. A. Suthers and T. Fitch), pp. 83-117. New York: Springer Handbook of Auditory Research.

Clark, C. J. and Dudley, R. (2010). Hovering and forward flight energetics in Anna's and Allen's Hummingbirds. *Physiol. Biochem. Zool.* **83**, 654-662.

Clark, C. J. and Mistick, E. A. (2018). Strategic acoustic control of a hummingbird courtship dive. *Curr. Biol.* **28**, 1257-1264.

Clark, C. J., Elias, D. O. and Prum, R. O. (2011a). Aeroelastic flutter produces hummingbird feather songs. *Science* **333**, 1430-1433.

Clark, C. J., Feo, T. J. and Escalante, I. (2011b). Courtship displays and natural history of the Scintillant (*Selasphorus scintilla*) and Volcano (*S. flammula*) hummingbirds. *Wilson J. Ornithol.* **123**, 218-228.

Clark, C. J., Feo, T. J. and Bryan, K. B. (2012). Courtship displays and sonations of a male Broad-tailed×Black-chinned Hummingbird hybrid. *Condor* **114**, 329-340.

Clark, C. J., Elias, D. O., Girard, M. B. and Prum, R. O. (2013a). Structural resonance and mode of flutter of hummingbird tail feathers. *J. Exp. Biol.* **216**, 3404-3413.

Clark, C. J., Elias, D. O. and Prum, R. O. (2013b). Hummingbird feather sounds are produced by aeroelastic flutter, not vortex-induced vibration. *J. Exp. Biol.* **216**, 3395-3403.

Clark, C. J., Kirschel, A. N. G., Hadjioannou, L. and Prum, R. O. (2016). *Smithornis* broadbills produce loud wing song by aeroelastic flutter of medial primary wing feathers. *J. Exp. Biol.* **219**, 1069-1075.

Clark, C. J., McGuire, J. A., Bonaccorso, E., Berv, J. S. and Prum, R. O. (2018). Complex coevolution of wing, tail, and vocal sounds of courting male bee hummingbirds. *Evolution* **72**, 630-646.

Debrouwere, M. (2013). An assessment of acoustically transparent wind tunnel walls for improving aero-acoustic measurements. *MSC thesis, Department of Aerodynamics, Delft University of Technology*.

Delacour, J. and Amadon, D. (1973). *Curassows and Related Birds*. New York: The American Museum of Natural History.

Dickinson, M. H., Lehmann, F.-O. and Sane, S. P. (1999). Wing rotation and the aerodynamic basis of insect flight. *Science* **284**, 1954-1960.

Dougherty, R. P., Ramachandran, R. C. and Raman, G. (2013). Deconvolution of sources in aeroacoustic images from phased microphone arrays using linear programming. *Int. J. Aeroacoust.* **12**, 699-718.

Feo, T. J. and Clark, C. J. (2010). The displays and sonations of the Black-chinned Hummingbird (Trochilidae: *Archilochus alexandri*). *Auk* **127**, 787-796.

Grinnell, J. (1929). A new race of hummingbird from southern California. *Condor* **31**, 226-227.

Hingee, M. and Magrath, R. D. (2009). Flights of fear: a mechanical wing whistle sounds the alarm in a flocking bird. *Proc. R. Soc. Biol. Sci. Ser. B* **276**, 4173-4179.

Hunter, T. A. (2008). On the role of wing sounds in hummingbird communication. *Auk* **125**, 532-541.

Hunter, T. A. and Picman, J. (2005). Characteristics of the wing sounds of four hummingbird species that breed in Canada. *The Condor* **107**, 570-582.

Miller, S. J. and Inouye, D. W. (1983). Roles of the wing whistle in the territorial behavior of male Broad-tailed Hummingbirds (*Selasphorus platycercus*). *Anim. Behav.* **31**, 689-700.

Niese, R. L. and Tobalske, B. W. (2016). Specialized primary feathers produce tonal sounds during flight in rock pigeons (*Columba livia*). *J. Exp. Biol.* **219**, 2173-2181.

Norberg, R. Å. (1991). The flappet lark *Mirafra rufocinnamomea* doubles its wingbeat rate to 24hz in wing-clap flight display: a sexually selected feat. *J. Exp. Biol.* **159**, 515-523.

Otte, D. (1970). A comparative study of communicative behavior in grasshoppers. *Miscellaneous Publications of the Museum of Zoology* **141**, 1-168.

Remillieux, M. C., Crede, E. D., Camargo, H. E., Burdisso, R. A., Devenport, W. J., Rasnick, M., Seeters, P. V. and Chou, A. (2008). Calibration and demonstration of the new Virginia Tech anechoic wind tunnel. In 4th AIAA CEAS Aeroacoustics Conference, Vancouver, Canada.

Sarradj, E., Fritzsche, C., Geyer, T. and Giesler, J. (2009). Acoustic and aerodynamic design and characterization of a small-scale aeroacoustic wind tunnel. *Appl. Acoust.* **70**, 1073-1080.

Soderman, P. T. and Allen, C. S. (2002). Microphone measurements in and out of airstream. In *Aeroacoustic Measurements* (ed. T. J. Mueller), pp. 1-61. New York: Springer.

Sueur, J., Tuck, E. J. and Robert, D. (2005). Sound radiation around a flying fly. *J. Acoust. Soc. Am.* **118**, 530-538.

Tobalske, B. W., Warrick, D. R., Clark, C. J., Powers, D. R., Hedrick, T. L., Hyder, G. A. and Biewener, A. A. (2007). Three-dimensional kinematics of hummingbird flight. *J. Exp. Biol.* **210**, 2368-2382.

Yack, J. E., Otero, L. D., Dawson, J. W., Surlykke, A. and Fullard, J. H. (2000). Sound production and hearing in the blue cracker butterfly *Hamadryas feronia* (Lepidoptera, Nymphalidae) from Venezuela. *J. Exp. Biol.* **203**, 3689-3702.
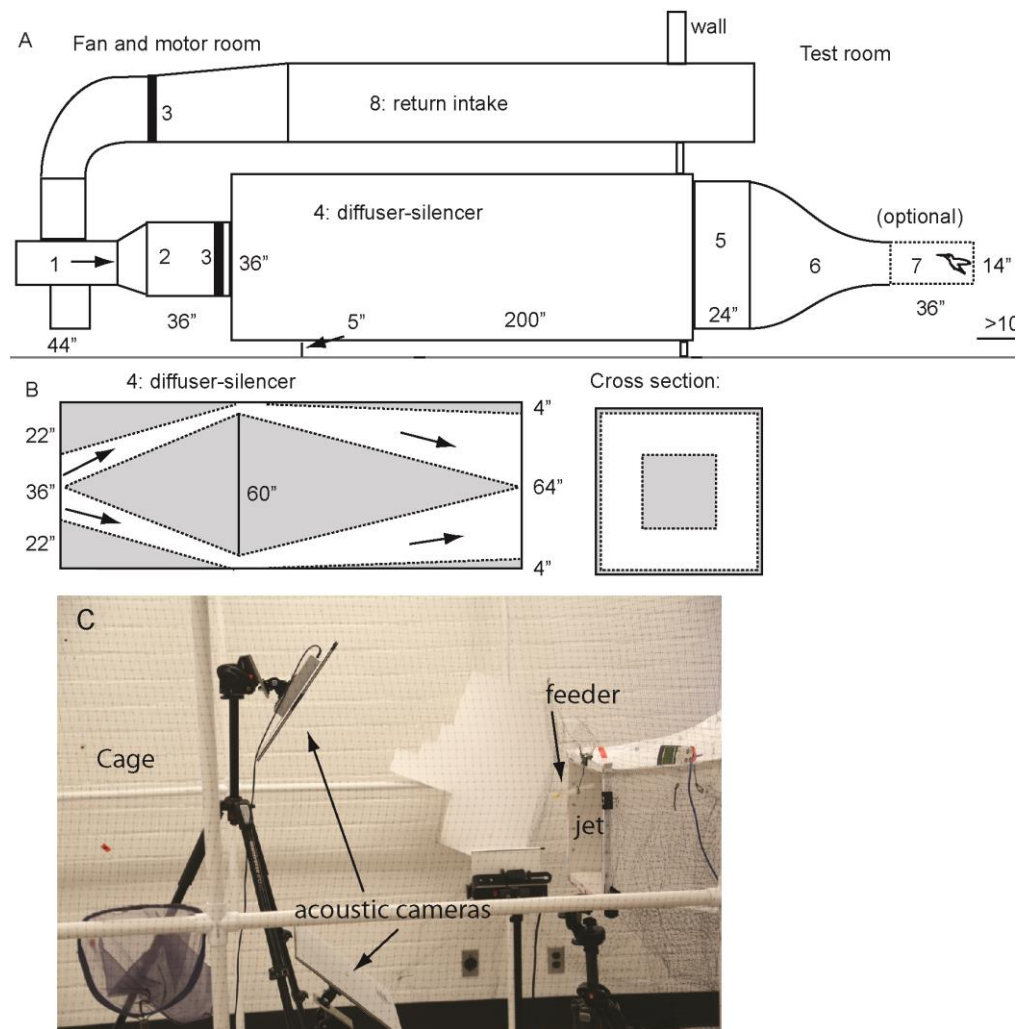
Figure S1. The aeroacoustic wind tunnel. **A**) Air flows out of the centrifugal fan (1) into a duct (2), through a vibration isolation boot (3) and into the diffuser-silencer. The settling chamber (5) contained a 4" honeycomb (hole diameter: 0.2") and then three pressure screens (open area: 64%) each separated by 4". 6: the contraction section, and 7: an optional working section (not used in the present study). Air then enters the open lab, with slightly more than 100" of space until striking a wall, when the optional working section is attached. There is a wall separating the test room from the fan and motor room. **B**) Interior of the diffuser-silencer. Grey areas are filled with recycled cotton batting. Suspended in the middle of the diffuser silencer is an insert that prevents direct transmission of sound from the fan to the test section, which the air (arrows) flows around. **C**) Image of the jet and part of the experimental setup. Note: acoustic cameras are in a different orientation than was used in present study. (1" is 2.54 cm).
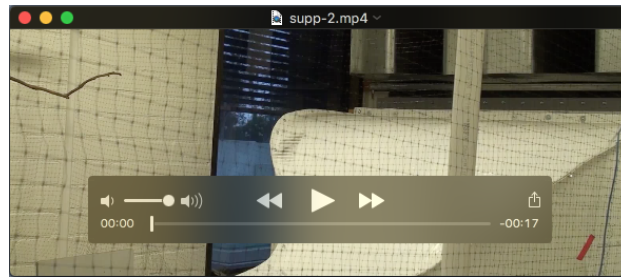
Movie 1. Adult Male Allen's Hummingbird (*Selasphorus sasin*) wing trill. Flight is inside the cage used in the experiment.

Movie 2. Acoustic camera video of a male Allen's hummingbird as it visits the feeder at an airspeed of 0 m s⁻¹. Note: heat map auto-scales (range: 20 dB), unlike in videos used to make Figs. 5, 6.

Movie 3. Acoustic camera video of a male Allen's hummingbird as it visits the feeder at an airspeed of 14 m s⁻¹. Heat map auto-scales (range: 20 dB). Note self-noise of feeder.